Mechanistic and Kinetic Study of the ATP-Dependent DNA Ligase of *Neisseria meningitidis*†

Sophie Magnet and John S. Blanchard*

Department of Biochemistry, Albert Einstein College of Medicine, 1300 Morris Park Avenue, Bronx, New York 10461

Received August 27, 2003; Revised Manuscript Received November 12, 2003

ABSTRACT: The gene from *Neisseria meningitidis* serogroup A, encoding a putative, secreted ATP-dependent DNA ligase was cloned and overexpressed, and the soluble protein was purified. Mass spectrometry indicated that the homogeneous protein was adenylated as isolated, and sedimentation velocity experiments suggested that the enzyme exists as a monomer in solution. The 31.5 kDa protein can catalyze the ATP-dependent ligation of a singly nicked DNA duplex but not blunt-end joining. The first step of the overall reaction, the ATP-dependent formation of an adenylated ligase, was studied by measuring the formation of the covalent intermediate and isotope exchange between [α-^{32}P] ATP and PP_i. Mg^{2+} was absolutely required for this reaction and was the best divalent cation to promote catalysis. Electrophoretic gel mobility shift assays revealed that the enzyme bound both unnicked and singly nicked double stranded DNA with equivalent affinity ($K_d \sim 50$ nM) but cannot bind single stranded DNA. Preadenylated DNA was synthesized by transferring the AMP group from the enzyme to the 5′-phosphate of a 3′-dideoxy nicked DNA. The rate of phosphodiester bond formation at the preadenylated nick was also Mg^{2+}-dependent. Kinetic data showed that the overall rate of ligation, which occurred at 0.008 s^{-1}, is the result of three chemical steps with similar rate constants (≈0.025 s^{-1}). The K_m values for ATP and DNA substrates, in the overall ligation reaction, were 0.4 μM and 30 nM, respectively.

DNA ligases are ubiquitous enzymes involved in the maintenance and the evolution of the genotype of the cell because of the essential role that they play in replication, recombination, and DNA repair (*2*, *3*). They vary in size from 30 to 100 kDa, with a low level of overall sequence conservation outside of the six sequence motifs constituting the active site of the enzymes (*4*−*7*). Structural data reveal that despite this sequence diversity, DNA ligases, as well as other nucleic acid modifying enzymes belonging to the nucleotidyl transferase superfamily (*8*), share a common basic structural core that includes the conserved motifs of DNA ligases (*7*). This core can be divided into two structural domains, the adenylylation domain that binds and reacts with the AMP donor substrate and the OB domain involved in DNA recognition and binding (*7*). The common core appears to be responsible for a common mechanism for catalysis of the joining of breaks in duplex DNA shared by all DNA ligases, whereas the additional N- or C-terminal domains are proposed to be involved in more specific DNA/protein or protein/protein interactions responsible for pathway specificity (*7*, *9*, *10*).

The mechanism of the overall DNA ligation reaction can be divided into three catalytic steps involving two covalent intermediates (*11*). The first step involves the attack of the ε-amino group of a Lys residue, located in motif I, on the adenylyl phosphorus of either NAD^+ or ATP, to form a covalent phosphoamide linkage between protein and AMP and releasing either NMN or PP_i, respectively. In the second step, the adenylated protein intermediate transfers the AMP moiety to the 5′-phosphoryl group at the DNA break site to form, via a new pyrophosphate linkage, the adenylated DNA intermediate. In the final step, the enzyme catalyzes the formation of a phosphodiester bond between the 3′-hydroxyl group and the 5′-adenylated phosphate of the DNA, releasing AMP.

DNA ligases are divided into two classes depending on the identity of the AMP donor, NAD^+ or ATP, that they use in the first step. The main difference between the two classes of enzymes is the presence of an extra N-terminal domain (domain Ia) in the NAD^+-dependent DNA ligases (*7*). This domain is essential for NAD^+-dependent adenylylation and AMP transfer to a 5′-phosphate nick (*12*). Until recently, it was believed that ATP-dependent DNA ligases were found only in eucaryotes, viruses, and archeabacteria and that NAD^+-dependent DNA ligases were found specifically in eubacteria. In the past decade, the sequences of many bacterial genomes have revealed that some of them, in addition to the structural gene(s) for the typical bacterial NAD^+-dependent DNA ligase(s), also contain gene(s) predicted to encode ATP-dependent DNA ligase(s) based on sequence homology (*6*). Reciprocally, a NAD^+-dependent DNA ligase was recently characterized from a eukaryotic virus (*13*).

Since the early detailed mechanistic characterization of both the bacteriophage T4 ATP-dependent and the *Escherichia coli* NAD^+-dependent DNA ligases (*11*, *14*), several DNA ligases from all kingdoms of life have been characterized (*3*, *15*−*17*). Among the putative bacterial ATP-dependent DNA ligases identified, only two have been

† This work was supported by NIH Grant AI33696.

* Corresponding author. Phone: (718) 430-3096. Fax: (718) 430-8565. E-mail: blanchar@aecom.yu.edu.

10.1021/bi0355387 CCC: $27.50 © 2004 American Chemical Society
Published on Web 12/31/2003

functionally characterized, and they have revealed very distinct features. In 1997, Cheng et al. showed that *Haemophilus influenzae* encoded a 31 kDa protein able to form a protein-AMP intermediate using ATP and to catalyze a strand joining at a singly nicked DNA duplex (*18*). In 2002, Weller et al. demonstrated that the 83.6 kDa polypeptide encoded by Rv0938 from *Mycobacterium tuberculosis* has the ability of self-adenylylation in the presence of ATP and is involved in double-strand break joining (*19*). This activity was found to be strongly activated by another protein component, a bacterial Ku homodimer, similar to the nonhomologous end-joining pathway of eukaryotic cells (*19*). Very little is known about the physiological role of ATP-dependent DNA ligases in bacteria. The *Bacillus subtilis* homologue of Rv0938, ykoV, which was proposed to be involved in the repair of DNA damage due to ionizing radiation, was shown to be neither essential nor able to substitute for the NAD^+-dependent DNA ligase of the same species, yerG (*20*). Other studies have shown that heterologous complementation between ATP- and NAD^+-dependent enzymes is possible (*21*, *22*).

In this study, we have cloned and expressed the structural gene of the putative ATP-dependent DNA ligase of *Neisseria meningitidis* (ADL). We have purified the protein and investigated its substrate specificity and kinetic properties. The results permit us to highlight the similarities, as well as the differences, between ADL and both NAD^+-dependent bacterial DNA ligases and various ATP-dependent DNA ligases.

EXPERIMENTAL PROCEDURES

Cloning and Expression of the adl Gene. The *adl* gene (ATP dependent DNA ligase) was amplified from genomic DNA of *N. meningitidis* serogroup A, ATCC 53417D, using *Pfu* DNA polymerase and the primers C1: 5′-GGATTC-CATATGATTAAGAAGACAATCGGC-3′ and C2, containing a six-His tagged coding region (bold characters): 5′-CCCAAGCTTTTA**ATGGTGATGGTGATGGTG**GC GGTCGGTACGCACGCGC-3′, complementary to the 5′-terminal coding strand and to the 3′-terminal noncoding strand of the NMA0388 open reading frame of *N. meningitidis* Z2491, respectively. The amplification product was restricted with *Nde*I and *Hind*III (restriction sites underlined in the PCR primer sequences) and ligated into the pET23a-(+) expression vector (Novagen). A recombinant plasmid obtained from a transformant of *E. coli* BL21(DE3)pLysS (Novagen) selected on Luria Broth (LB) agar containing 100 μg/mL of ampicillin and 35 μg/mL of chloramphenicol was used as template to determine the sequence of the DNA insert[1] by the dideoxynucleotide chain termination method. A single colony of this transformant was used to inoculate 1 L of LB containing selective antibiotics and grown at 37 °C until the optical density at 600 nm reached 1. The expression of the *adl* gene was then induced by the addition of 0.3 mM isopropyl-β-D-thiogalactoside (IPTG) to the culture, which was grown for an additional 4 h. After cell lysis, the supernatant and the pellet of the crude extract were analyzed separately by sodium dodecyl sulfate−polyacrylamide gel electrophoresis (SDS−PAGE) using 10−15% Phastgels (Amersham Pharmacia).

[1] GenBank Accession Number AY356550.

Protein Purification. Twenty-five grams of *E. coli* BL21-(DE3)pLysS/pET23a(+)::*adl-His*$_6$, recovered by centrifugation from a 10 L culture grown as described previously, were suspended in 40 mL of 20 mM triethanolamine hydrochloride (TEA) pH 7.8, containing one Complete Protease Inhibitor Cocktail tablet (Roche) and 1.6 M NaCl. The cells were lysed by ultrasonic disruption for 10 min, and the crude extract was stirred for 1 h at 4 °C in the high salt buffer. Cell debris was separated from the soluble fraction by a 45 min ultracentrifugation at 35 000 rpm. The clear supernatant was diluted to 80 mL with 20 mM TEA, pH 7.8 and applied to a column containing 50 mL of Ni-NTA His.Bind resin (Novagen) equilibrated with 20 mM TEA, pH 7.8 containing 300 mM NaCl. Proteins were eluted at 1 mL/min with a linear 0−250 mM imidazole gradient. The fractions eluting between 100 and 175 mM imidazole, which contained a single band (>95%) with a molecular mass estimated at 30 kDa by SDS−PAGE, were pooled and dialyzed against 50 mM HEPES, pH 7.5 containing 200 mM NaCl, 1 mM dithiothreitol (DTT), and 0.1 mM EDTA, for 2 h. After clearing of the minor precipitate formed during dialysis by centrifugation, the protein was concentrated and stored at −20 °C in 50% glycerol.

Deadenylylation of the Ligase. Three nmol of ADL were incubated in 600 μL of 50 mM HEPES, pH 7.5 containing 5 mM DTT, 10 mM $MgCl_2$, 50 mM NaCl, and 1 mM PP_i for 45 min at room temperature. The deadenylated ligase was purified by applying the reaction mixture to a 6 mL Sephadex G-10 column, preequilibrated with 50 mM HEPES, pH 7.5 containing 50 mM NaCl. The products of the reaction were eluted with the same buffer, and protein-containing fractions were detected by the absorbance at 280 nm. The protein obtained was subjected to mass spectrometry analysis and stored at −20 °C in 50% glycerol.

Analytical Methods. The protein concentration was estimated by the Bio-Rad protein assay method using bovine serum albumin as a standard. The molecular mass of the protein was determined by MALDI and electrospray ionization-mass spectrometry (Laboratory for Macromolecular Analysis and Proteomics (LMA&P), Albert Einstein College of Medicine, NY). An estimate of the native molecular weight of ADL-His_6 was determined by measuring the sedimentation velocity of the protein at three different concentrations by analytical ultracentrifugation (LMA&P, Albert Einstein College of Medicine, NY).

DNA Substrates. The oligodeoxynucleotides (Table 1) used to prepare DNA substrates or ligands were obtained from Invitrogen with the exception of O8 (3′-dideoxy), which was purchased from Qiagen. Oligodeoxynucleotides (Table 2) were 5′-^{32}P-labeled using 1 unit of T4 polynucleotide kinase per 5 pmol of oligodeoxynucleotide and a 4-fold excess of 30−100 Ci/mmol [γ-^{32}P] ATP as previously described (*23*) and purified by gel filtration using MicroSpin G-25 Columns (Amersham Biosciences). Complementary oligodeoxynucleotides were then annealed to form the DNA substrates or ligands listed in Table 2. The adenylated-5′-^{32}P-labeled O1 was prepared by incubating S6, double stranded DNA containing a 3′-dideoxy single nick (Table 2) with 0.2 μM ADL for 48 h in 50 mM HEPES, pH 7.5 containing 5 mM DTT, 10 mM $MgCl_2$, 50 mM NaCl, and 100 μM ATP. The adenylated-5′-^{32}P-labeled O1 oligodeoxynucleotide was purified by gel electrophoresis as previously described (*23*). The

Table 1: Oligodeoxynucleotides Used to Generate DNA Substrates

name	nucleic acid sequence (from 5′ to 3′)	length
O1	TCAGACCTGCAGGCGTTCCC	20
O2	CGAGTCATGTGCCGTGAGCC	20
O3	GGGAACGCCTGCAGGTCTGAGGCTCACGGCACATGACTCG	40
O4	CGAGTCATGTGCCGTGAGCCTCAGACCTGCAGGCGTTCCC	40
O5	CGAGTCATGTGCCGTGAGCG	20
O6	CTATGGGAACGCCTGCAGGT	20
O7	CTGAGGCTCACGGCACATGACTCGACTTTA	30
O8	CGAGTCATGTGCCGTGAGC[ddC]	20
O9	CGAGTCATGTGCCGTGAGC	19

Table 2: DNA Substrates or Ligands Used in This Study[a]

Name	Composition	Description	Scheme
S1	O2,O1* + O3	double strand singly nicked	
S2	O5,O1* + O3	double strand singly nicked, 3' nick mismatched	
S3	O3*	unicked single strand	
S4	O4* + O3*	double stranded unicked	
S5	O2,O1* + O6,O7*	double stranded doubly nicked	
S6	O9,O1* + O3	double strand singly nicked, 3' nick dideoxy	
S7	O2,O1*AMP + O3	double strand singly nicked, 5'-preadenylated	
S8	O9,O1* + O3	double strand singly nicked, 3'-gap	

[a] *: ^{32}P-label.

concentration of DNA substrates was determined by measuring the radioactivity using liquid scintillation counting.

DNA Binding Experiments. Binding isotherms were obtained from electrophoretic gel mobility shift assays (EMSA). Various amounts of enzyme (0−1 μM) were incubated in 50 mM HEPES, pH 7.5 containing 0−200 mM NaCl, 5 mM DTT with 1 nM DNA ligand, for 30 min at 25 °C. The samples were then loaded onto a 6% TBE polyacrylamide gel. The amount of free DNA was quantified (*24*) by autoradiography, and the data were fitted to the Hill equation: $F = u + (l - u)((1/K_d)^h x^h)/(1 + (1/K_d)^h x^h))$ where F is the amount of free DNA, x is the concentration of enzyme, h is the Hill coefficient, and u and l are the upper and lower limits of the Y axis, respectively.

Kinetic Reaction Conditions. Unless specifically noted in the text, reactions were performed at 25 °C in 50 mM HEPES, pH 7.5 containing 50 mM NaCl, 5 mM DTT, and 10 mM $MgCl_2$. Reactions were initiated by the addition of enzyme and quenched by the addition of 0.1 M EDTA and SDS buffer.

Adenylylation Reaction. Reaction mixtures for determining the kinetics of adenylylation contained 5−200 μM [α-^{32}P] ATP (15 Ci/mmol) and 1 μM deadenylated ligase. The samples were boiled and resolved by SDS−PAGE on 12% polyacrylamide gels, and the [^{32}P]-adenylated ligase was quantified by autoradiography. The determined rate of adenylylation corresponds to the first-order rate constant of the kinetic data fitted to a single exponential. The Mg^{2+} concentration dependence of the reaction was studied by measuring the amount of adenylated ligase in reaction mixtures containing 200 μM [α-^{32}P] ATP and from 0 to 20 mM $MgCl_2$, incubated for 4 min. To study the dependence of the reaction on the identity of the divalent cation, DTT was omitted from the reaction mixtures.

Isotope Exchange. The reversibility of the adenylylation step was studied by measuring the rate of isotope exchange between [γ-^{32}P] ATP and PP_i. Kinetic analysis was performed in the presence of 0.1−0.5 μM ligase at a fixed concentration of one substrate (5 μM [γ-^{32}P] ATP or 50 μM PP_i), while the concentration of the second was varied (0.5−50 μM [γ-^{32}P] ATP and 3−200 μM PPi). Samples were spotted onto PEI-cellulose F thin-layer chromatography (TLC) plates (EM-Sciences) and developed with 0.5 M ammonium bicarbonate. The respective amounts of [γ-^{32}P] ATP and [^{32}P] PPi were quantified by autoradiography. The initial rate of isotope exchange was determined by plotting ([^{32}P]PP_i/([^{32}P]PP_i + [γ-^{32}P]ATP))[γ-^{32}P]ATP/[ADL] versus time.

Phosphodiester Bond Formation Assay. The rate of phosphodiester bond formation was determined by single turnover experiments performed in 10 μL reactions containing 50 nM substrate S7 and 600 nM deadenylated ligase. After boiling, the samples were loaded onto a denaturing 1.2 X TBE, 7 M urea, 18% polyacrylamide gel. The dependence of this catalytic step on Mg^{2+} concentration was investigated by quantification of the different DNA species (20 , 21 , and 40 mer) present in the mixture after a 1 min reaction in the presence of 0−200 mM $MgCl_2$.

Overall Ligation Assay. To investigate the substrate specificity of the enzyme, various substrates were incubated overnight, in the presence of 100 μM ATP and 0.1 μM ADL or T4 DNA ligase as a positive control. To study the substrate concentration dependence of the initial rate of the ligation reaction, steady-state kinetics (0−10 min) was performed either in the presence of 1 nM ADL, a fixed and saturating concentration of ATP (100 μM), and various amounts of S1 DNA substrate (20−400 nM), or in the presence of 10 nM ADL, a fixed and saturating concentration of S1 DNA substrate (450 nM) and various concentrations of ATP (0.2−50 μM). The reaction samples were boiled and resolved on denaturing 1.2 X TBE, 7 M urea, 13% polyacrylamide gel. The initial velocity was obtained by plotting (40 mer/(40 mer + 20 mer))[S1]/[ADL] versus time.

Autoradiography, Quantification, and Data Analysis. Dried gels and TLC plates were exposed to an imaging screen, which was scanned using a STORM 820 phosphoimager (Amersham Pharmacia Biotech). The different labeled species were quantitated using the ImageQuant 5.2 software, and the data were fitted using the SigmaPlot 6.0 programs.

Reagents. All DNA restriction and modifying enzymes were purchased from New England Biolabs, ampicillin and chloramphenicol were from Sigma, LB and IPTG were from Fisher, and [α or γ -^{32}P] ATP was from Perkin-Elmer Life Sciences.

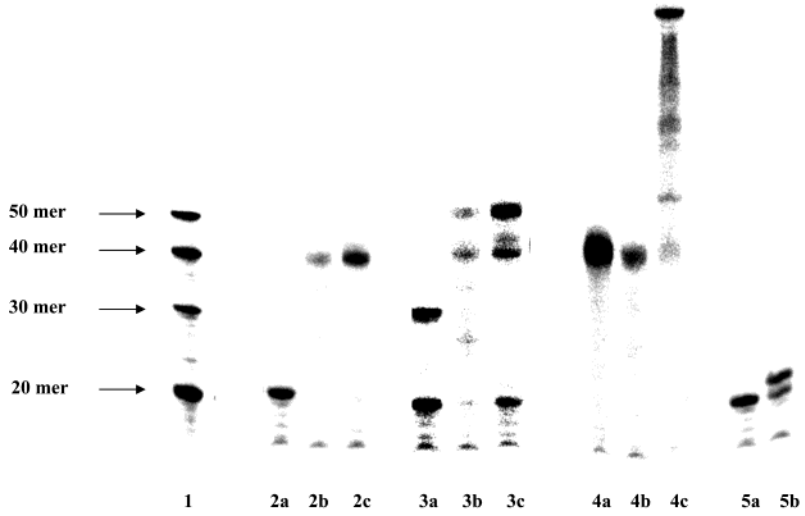

FIGURE 1: Substrate specificity of ADL. Autoradiograph of ligation reactions separated on a denaturing TBE polyacrylamide gel. Lane 1: molecular weight marker. Substrate S1 (lanes 2), S5 (lanes 3), S4 (lane 4), or S6 (lanes 5) was incubated overnight as described in the Experimental Procedures without enzyme (a), with ADL (b), or with T4 DNA ligase (c). The size of the substrates and products are indicated.

RESULTS

Purification and Physical Characteristics of the Recombinant ADL-His$_6$ Protein. The *adl* gene amplified from genomic DNA of *N. meningitidis* serogroup A, ATCC 53417, was cloned into the expression vector pET23a(+). The 825 bp sequence of this gene[1] was determined and found to be 96% identical to the NMA0388 open reading frame of the sequenced Z2491 strain, used to design PCR primers. The deduced encoded ADL protein differed from the homologous published sequence, annotated as a putative, secreted ATP-dependent DNA ligase, by four amino acids located outside the conserved motifs of DNA ligases (E37 instead of D37, V60 instead of I60, V65 instead of A65, and A103 instead of V103). The corresponding histidine-tag recombinant protein had a calculated isoelectric point of 10 and a molecular weight of 31 548 Da. The conditions of expression described in the experimental procedures yielded a considerable amount of enzyme, but 90% was present in the insoluble cell pellet. Induction of protein expression at a lower temperature did not improve the protein solubility, although suspension of the cells in 1.6 M NaCl increased the recovery of soluble protein. The protein was purified to homogeneity (>95%) in one step by nickel affinity chromatography. The native molecular weight of the purified recombinant protein was estimated at different protein concentrations between 30 and 32 kDa by analytical ultracentrifugation, suggesting that the enzyme exists as a monomer in solution. Mass spectrometry confirmed the homogeneity of the preparation and indicated a subunit molecular mass of 31 873 Da as compared to the theoretical value of 31 548. Since the mass of AMP is 330 Da, these data suggested that greater than 90% of the purified protein was adenylated. A molecular mass of 31 543 Da was determined for the protein preincubated in the presence of Mg^{2+} and pyrophosphate and then purified by gel filtration chromatography. This result confirmed the adenylation state of the purified, heterologously expressed recombinant ADL and demonstrated that a homogeneous nonadenylated protein can be successfully prepared.

DNA Substrate Specificity. The DNA substrate specificity of ADL was investigated by carrying out overnight reactions. The results presented in Figure 1 show that ADL is able to catalyze the sealing of a single nick in a duplex DNA molecule, probed by the conversion of a labeled 20 mer to a labeled 40 mer using S1 as substrate (Table 2). In the reaction using S5 as substrate (Table 2), both labeled 20 mer and labeled 30 mer were converted to labeled 40 and 50 mer, indicating that nicks on both strands of the duplex can be efficiently sealed. The lack of 39 or 40 mer products in the reaction containing S8 or S2 substrate (Table 2), respectively, indicated that the ligase activity did not tolerate either a G/G mismatch or a gap at the 3′-extremity of the nick (data not shown). As expected, the 3′-OH is absolutely required for the formation of the phosphodiester bond but not for the binding to the ligase or adenyl transfer to the DNA since the labeled 20 mer of S6 (Table 2) was partially converted into labeled 21 mer. In contrast to T4 DNA ligase, which exhibits blunt end joining activity as probed by the formation of labeled 40 mer concatemers from S4 (Table 2), the ADL ligase activity was found to be specific for nicked-DNA and was not able to catalyze blunt end joining even after prolonged incubation.

Adenylylation Reaction. The first step of the DNA ligation reaction, self-adenylylation of the enzyme, was first studied by measuring the formation of a covalent protein-adenylate intermediate resulting from the adenyl transfer from [α-^{32}P] ATP to deadenylated ADL. The kinetics performed in the presence of 10 mM $MgCl_2$ and from 1 to 200 μM ATP led to similar fits. The very small changes observed for the first-order rate constants obtained did not correlate with [ATP], suggesting that 1 μM ATP was saturating. The mean of these first-order rate constants provided a rate (k_1) of 0.026 ± 0.006 s^{-1} for the ADL self-adenylylation step (Supporting Information). A very faint signal was detected after a 90 min reaction in the presence of 1 μM [^{32}P] NAD^+ (<0.1% of the signal obtained with 1 μM [α-^{32}P] ATP), demonstrating the specificity of ADL for ATP as AMP donor. No intermediate was detected in the absence of Mg^{2+}, revealing that the

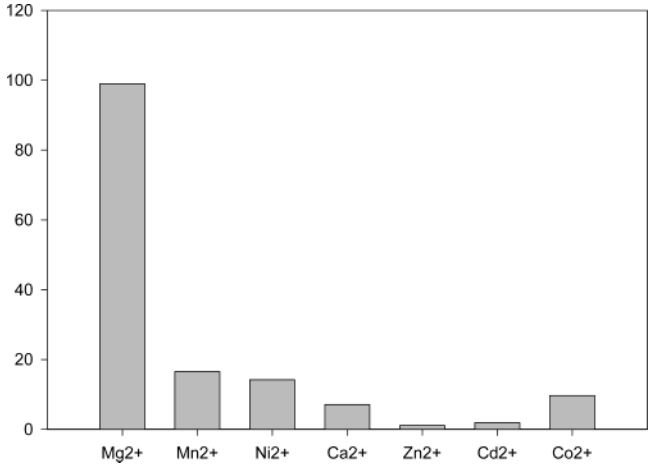

FIGURE 2: Dependence of the adenylylation reaction on the identity of the metal cation. The bars represent the percentage of adenylated ligase after a 20 min reaction in the presence of 10 mM of each different metal cation indicated as compared to the amount of adenylated ligase obtained in the same time in the presence of 10 mM $MgCl_2$ (arbitrarily defined as 100%). Reactions were performed in the presence of 100 μM ATP and in the absence of DTT.

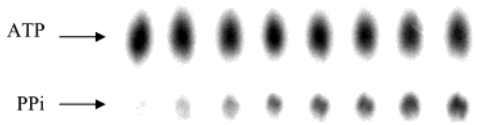

FIGURE 3: Isotope exchange catalyzed by ADL. Autoradiograph of isotope exchange reactions separated on a TLC plate. Reaction mixtures contained 0.5 μM ADL, 5 μM [γ-^{32}P] ATP, and 10 μM PP_i. The positions of ATP and PP_i are indicated.

divalent metal cation is absolutely required for this step. The Mg^{2+} concentration requirement for the self-adenylylation was investigated and showed that the reaction occurs at an optimal Mg^{2+} concentration of 2 mM (data not shown). To study the dependence of the reaction on the identity of the divalent cation, DTT was omitted from the reaction mixtures to avoid precipitation of the metals. The results shown in Figure 2 indicated that Mg^{2+} is by far the best metal ion for this reaction among the metals tested.

To study the reversibility of the first step, we measured isotope exchange between [γ-^{32}P] ATP and PP_i. The kinetics of isotope exchange (Figure 3) were obtained in the presence of various concentrations of ATP and PP_i. The maximal rate of isotope exchange (k_{ex}), 0.006 $\pm$ 0.0002 s^{-1}, and the concentration of PP_i that gave a rate equal to one-half of k_{ex}, 22 $\pm$ 8 μM, were determined from the reciprocal plot of the kinetics performed at a saturating concentration of ATP (5 μM) and various concentrations of PP_i (Supporting Information).

DNA Binding. DNA binding studies were performed by EMSA with four different DNA ligands: S1, a perfectly matched DNA duplex containing a single nick; S2, a DNA duplex containing a G/G 3′-mismatched single nick; S3, a single strand DNA; and S4, a unnicked DNA duplex. No complex formation was observed with the single stranded S3, but the three duplex DNA ligands were able to form a complex with the ADL protein, located in the wells of the gel. The data were analyzed by measuring the disappearance of the free DNA substrate as a function of [ADL] (*24*). The K_d values of 46 $\pm$ 1, 46 $\pm$ 1, and 55 $\pm$ 1 nM determined for

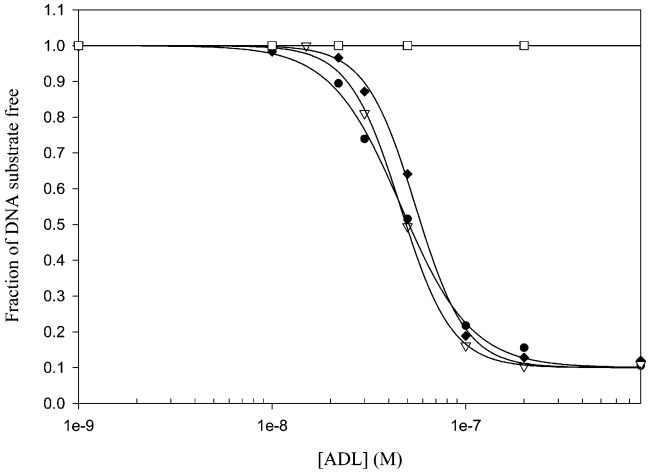

FIGURE 4: DNA binding by ADL. Data from EMSA were fitted to the Hill equation. DNA ligand used are (●) S1; (◆) S2; (□) S3; and (▽) S4 (Table 2).

S1, S2, and S4, respectively (Figure 4), demonstrated that ADL bound the three double stranded DNA ligands with equivalent affinity. The Hill coefficients were greater than 1 in all cases (between 2.4 and 3.3), suggesting that more than one molecule of protein is bound per molecule of DNA. Thus, the large size of the complex resulting from the oligomerization of the protein onto the DNA is the likely reason for its inability to penetrate into the gel. The experiments were repeated in the presence of 100 and 200 mM KCl to ensure that the ADL-DNA complexes observed were not the result of nonspecific, ionic interactions between nucleic acids and very basic ADL protein (pI = 10). The presence of 200 mM salt resulted in a similar and expected shift of the sigmoid binding curve ($K_d \approx$ 300 nM) for all three ligands but did not affect either the Hill coefficient values or the ability of the complexes to enter into the gel (data not shown).

AMP Transfer to DNA and Phosphodiester Bond Formation at a 5′-Preadenylated Nick. The 5′-preadenylated O1 oligodeoxynucleotide used to make S7 substrate was prepared by transferring the AMP group from the adenylated ligase to the nonreactive S6 substrate (3′-dideoxy nick). Thus, the 3′-hydroxyl group of the nick is not required for either binding of the ligase or AMP transfer to the DNA. However, this reaction, carried out in the presence of 10 mM $MgCl_2$, was extremely slow, and after 48 h of incubation, only 65% of O1 was adenylated. By carrying out single turnover reactions with 20-fold excess enzyme over the 5′-preadenylated S7 substrate in the presence of 10 mM $MgCl_2$ (Figure 5A), a rate (k_3) of 0.022 $\pm$ 0.002 s^{-1} was determined for the phosphodiester bond formation step. The Mg^{2+} dependence of this last step was investigated by measuring the extent of phosphodiester bond formation during a one minute, single turnover reaction in the presence of 0−200 mM $MgCl_2$. As shown in Figure 5B, the reaction was strongly affected by the concentration of the metal ion. The optimum [Mg^{2+}] for the phosphodiester bond formation step, probed by the conversion of a labeled 21 mer to labeled 40 mer, was 20 mM. The presence of the metal was not absolutely required for activity since some product was detected in a longer reaction performed in the absence of $MgCl_2$ (data not shown), but very high concentrations of $MgCl_2$ (200 mM) abolished this activity, probably preventing ADL-DNA binding. In-

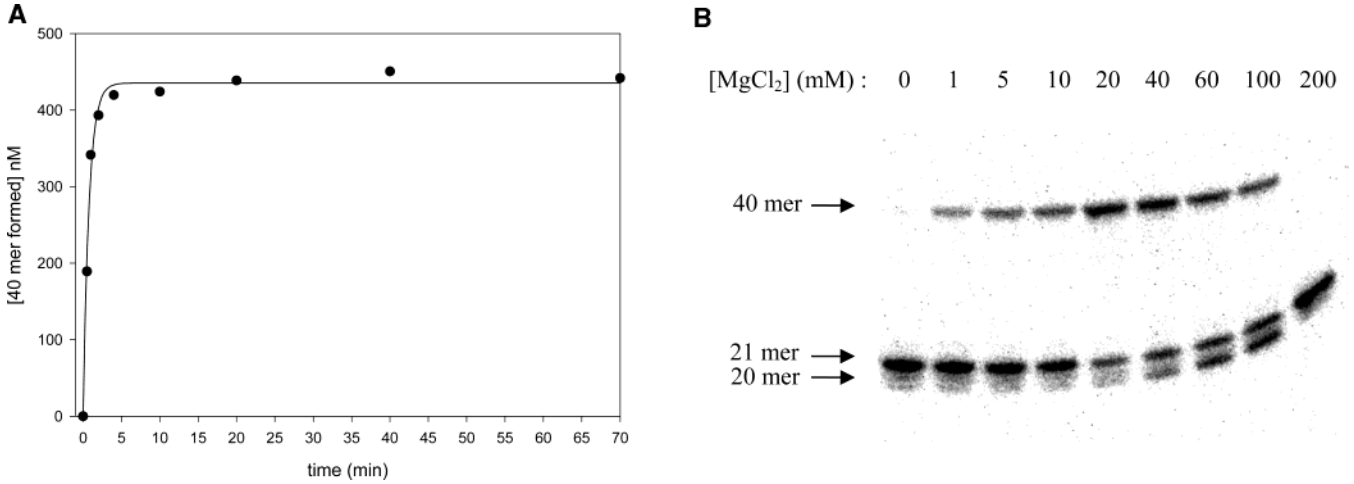

FIGURE 5: Single turnover phosphodiester bond formation catalyzed by deadenylated ADL. (A) Time course of product formation. The 10 μL reaction contained 600 nM ADL and 50 nM preadenylated-DNA substrate S7. (B) Dependence of the phosphodiester bond formation on $MgCl_2$ concentration. Reaction mixture components are described in the Experimental Procedures, and [$MgCl_2$] is indicated. Reactions were stopped after 1 min. The localizations of the 40, 21, and 20 mer are indicated.

terestingly, as the concentration of $MgCl_2$ increases from 20 to 100 mM, and only in the presence of enzyme, the amount of 40 mer product formed decreased, while the appearance of a 20 mer, corresponding to deadenylated O1, inversely increased. This result suggested that if the divalent cation is not required for catalysis, it might strongly affect the equilibrium between the enzyme adenylate intermediate and the sealed DNA product.

Ligation Assay. Steady-state kinetics of sealing the single nick of the S1 substrate (Table 2) were performed at a fixed and saturating concentration of one substrate while the concentration of the second substrate was varied. The double reciprocal plot obtained at a saturating concentration of ATP (100 μM) and various concentrations of S1 allowed for the calculation of a k_{cat} value of 0.0085 $\pm$ 0.0018 s^{-1} for the overall ligation reaction and a K_m value for S1 of 29 $\pm$ 10 nM (Supporting Information). The initial velocity of ligation, obtained from kinetics performed at a fixed concentration of DNA substrate (400 nM) and various amounts of ATP (0.2−100 μM) allowed us to estimate the K_m of ATP at 0.4 $\pm$ 0.1 μM (Supporting Information).

DISCUSSION

The sequencing of several bacterial genomes has revealed the presence of open reading frames encoding putative ATP-dependent DNA ligases (*6*). The enzymatic activity of two of these has very recently been demonstrated. The ATP-dependent DNA ligase of *H. influenzae* catalyzes strand ligation of a singly nicked DNA duplex (*18*), while the Rv0938-encoded ligase of *M. tuberculosis*, related to ykoU from *B. subtilis*, has been shown to be involved in a nonhomologous end-joining pathway by interacting with a Ku homologue and catalyzing the joining of double strand breaks (*19*). The present study reports, for the first time, a detailed kinetic characterization of a bacterial ATP-dependent DNA ligase, ADL from *N. meningitidis*.

The size of the protein (31.5 kDa) and sequence homology revealed that ADL is related to the ATP-dependent DNA ligases of *H. influenzae*, *Campylobacter jejuni*, and *Vibrio* spp. with 64, 61, and 57% sequence similarity, respectively. Both PSORT WWW and SignalIP V2.0 servers predicted, with a probability greater than 0.9, that the DNA ligases mentioned previously contain an N-terminal signal sequence and a probable periplasmic space localization for the *N. meningitidis* and *H. influenzae* enzymes. Conversely, the *Mycobacterium* and *Pseudomonas* ATP-dependent DNA ligases, which share less homology with ADL (38% similarities) than the viral ATP-dependent DNA ligases, do not appear to contain such a signal sequence. Sedimentation velocity experiments showed that ADL is a monomer in solution, and mass spectrometry of the protein indicated that greater than 90% of the enzyme was purified in a preadenylated form. This observation is consistent with the kinetically determined values of ATP (<1 μM) and PP_i (22 μM) giving half of the maximal rate of the reversible adenylylation step and in vivo conditions, where the high [ATP] and the low [PP_i] would make this first step essentially irreversible.

The adenylylation reaction was specific for ATP and absolutely required the presence of Mg^{2+}. Mg^{2+} was not absolutely required for the phosphodiester bond formation from preadenylated DNA, but the rate for this step was influenced by the concentration of the metal ion. The optimal [$MgCl_2$] was 2 and 20 mM for the adenylylation and phosphodiester bond formation steps, respectively. A concentration of 10 mM Mg^{2+} was thus used for the kinetic studies of the three individuals steps as well as for the overall ligation reaction.

The formation of the enzyme-adenylate is readily reversible as demonstrated by isotope exchange. The rate of enzyme adenylylation (k_1 = 0.026 s^{-1}) and rate of isotope exchange (k_{ex} = 0.006 s^{-1}) allowed us to put a lower limit on k_{-1} of 0.006 s^{-1}, and the K_{eq} for this step is thus less or equal to 4.3. Single turnover experiments of phosphodiester bond formation at a preadenylated nicked DNA yielded a rate constant for this third step of 0.022 s^{-1}, and steady-state kinetics of the overall ligation yielded to an overall rate constant of 0.0085 s^{-1}. For a linear sequence of irreversible reactions steps, the reciprocal of the catalytic rate constant of the overall reaction is equal to the sum of the reciprocals of the rate constants of the partial steps of the reaction. Using this simplified model, we could calculate a

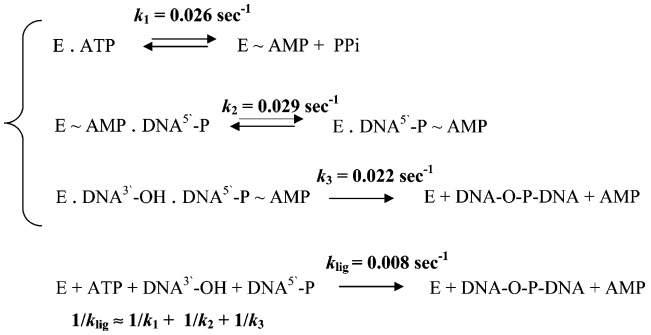

FIGURE 6: Scheme summarizing the kinetic data on the three individual steps and the overall ligation reaction catalyzed by ADL.

rate constant for the adenyl transfer from the adenylated protein to the DNA of 0.029 s^{-1} (Figure 6).[2] Given the standard errors associated with these values, all three steps occur at similar rates; thus, none of them appears to be significantly rate limiting. Given the similar chemical potentials of the substrates, products, and intermediates, this is perhaps not surprising. Adenyl transfer from the adenylated enzyme to a 3′-dideoxy singly nicked DNA duplex was very slow. The absence of the 3′-hydroxyl group could be responsible for the very slow rate of transfer either because it plays a undetermined role in catalysis of this second step or, more likely, because the adenylated DNA duplex-ADL complex dissociates very slowly.

The k_{cat} for the overall ligation catalyzed by the ATP-dependent DNA ligase of *N. meningitidis* (0.008 s^{-1}) is similar to those determined for the T4 ATP-dependent DNA ligase (0.0025 s^{-1}) (*14*) and the two *E. coli* NAD^+-dependent DNA ligases (0.02 s^{-1}) (*11*, *25*), although the k_{cat} value exhibited by the *E. coli* ligA can be increased 20-fold by the addition of NH_4^+ to reach a rate of 0.46 s^{-1}, similar to those estimated for the ATP-dependent DNA ligase of *Chorella* virus (0.16 s^{-1}) (*26*) and lig Tk of an archaeal (0.11 s^{-1}) (*27*).

Electrophoretic gel mobility shift assays showed that ADL specifically bound duplex DNA and not single stranded DNA. The protein exhibited essentially the same affinity for singly nicked and unnicked DNA duplex, indicating that the binding is not specific for the nick. This result is consistent with a Hill coefficient greater than 1, indicating the presence of multiple monomeric ligases in the protein-DNA complexes. The oligomerization of ADL on the DNA molecule suggests that the ligase binds nonspecifically to duplex DNA and moves along the nucleic acid molecule until a nick is found.

The ATP-dependent DNA ligase of *N. meningitidis* catalyzed the ligation of a singly nicked DNA duplex but not blunt end joining. It is becoming clear that for bacterial ATP-dependent DNA ligases, the genomic environment of the structural gene, the primary sequence, and in some cases, the enzymatic activity of the protein can be used to separate them into two classes. One class would include the ATP-dependent DNA ligases of *M. tuberculosis*, *B. subtilis*, *Mezorhizobium loti*, and *Pseudomonas aeroginusa*, which are between 70 and 94 kDa and consist of the basic core of the DNA ligases plus extra terminal domains. The presence of a Ku homologue determinant adjacent to their structural gene (*28*, *29*) suggests that they all exhibit a double strand joining activity as has been shown for the *M. tuberculosis* enzyme. The second class would include the ligases of *N. meningitidis*, *H. influenzae*, *C. jejuni*, and *Vibrio* sp. that (i) contain only the basic core of the DNA ligases with a size between 30.7 and 32.5 kDA, (ii) contain putative periplasmic proteins or membrane transporters in the genomic environment of the ligase gene, (iii) contain a predicted N-terminal signal sequence, and (iv) at least for the *N. meningitidis* and *H. influenzae* ligases, catalyze the ligation of a singly nicked DNA duplex. It is intriguing to speculate about the in vivo role of these latter ligases. Given the predicted periplasmic localization of the *N. meningitidis* and *H. influenzae* ligases and the fact that at least some strains of all the host species of this class of ligases are naturally competent for transformation (*30*), one could propose a potential role of these bacterial ATP-dependent DNA ligases in the transformation process. The oligomerization of ADL observed onto DNA duplex may suggest an additional role in protecting exogenous DNA from periplasmic nucleases (*31*).

[2] This is a simplification that allows for an estimate of the rate of the second reaction but does not implicitly consider the demonstrated reversibility of the first step and the likely reversibility of the second step. We can derive an exact equation for this model that does not allow us to calculate the net rate constants of all the steps (see Supporting Information for derivation 1 and the complete equation).

ACKNOWLEDGMENT

We thank A. Argyrou and M. Brenowitz for helpful discussions.

SUPPORTING INFORMATION AVAILABLE

Kinetic data for ADL adenylylation, isotope exchange, and overall ligation as well as the derivation of the rate equation for the reaction shown in Figure 6. This material is available free of charge via the Internet at http://pubs.acs.org.

REFERENCES

1. Cleland, W. W. (1975) *Biochemistry 14*, 3220−3224.
2. Timson, D. J., Singleton, M. R., and Wigley, D. B. (2000) *Mutat. Res. 460*, 301−318.
3. Tomkinson, A. E., and Levin, D. S. (1997) *Bioessays 19*, 893−901.
4. Sriskanda, V., and Shuman, S. (2002) *J. Biol. Chem. 277*, 9661−9667.
5. Sriskanda, V., and Shuman, S. (2002) *Nucleic Acids Res. 30*, 903−911.
6. Wilkinson, A., Day, J., and Bowater, R. (2001) *Mol. Microbiol. 40*, 1241−1248.
7. Doherty, A. J., and Suh, S. W. (2000) *Nucleic Acids Res. 28*, 4051−4058.
8. Shuman, S., and Schwer, B. (1995) *Mol. Microbiol. 17*, 405−410.
9. Doherty, A. J., and Wigley, D. B. (1999) *J. Mol. Biol. 285*, 63−71.
10. D. Timson, J., and Wigley, D. B. (1999) *J. Mol. Biol. 285*, 73−83.
11. Lehman, I. R. (1974) *Science 186*, 790−797.
12. Sriskanda, V., and Shuman, S. (2002) *J. Biol. Chem. 277*, 9695−9700.
13. Sriskanda, V., Moyer, R. W., and Shuman, S. (2001) *J. Biol. Chem. 276*, 36100−36109.
14. Hall, Z. W., and Lehman, I. R. (1969) *J. Biol. Chem. 244*, 43−47.
15. Wilkinson, A., Sayer, H., Bullard, D., Smith, A., Day, J., Kieser, T., and Bowater, R. (2003) *Proteins 51*, 321−326.
16. Sriskanda, V., Kelman, Z., Hurwitz, J., and Shuman, S. (2000) *Nucleic Acids Res. 28*, 2221−2228.

17. Kaczmarek, F. S., Zaniewski, R. P., Gootz, T. D., Danley, D. E., Mansour, M. N., Griffor, M., Kamath, A. V., Cronan, M., Mueller, J., Sun, D., Martin, P. K., Benton, B., McDowell, L., Biek, D., and Schmid, M. B. (2001) *J. Bacteriol. 183*, 3016−3024.
18. Cheng, C., and Shuman, S. (1997) *Nucleic Acids Res. 25*, 1369−1374.
19. Weller, G. R., Kysela, B., Roy, R., Tonkin, L. M., Scanlan, E., Della, M., Devine, S. K., Day, J. P., Wilkinson, A., d'Adda di Fagagna, F., Devine, K. M., Bowater, R. P., Jeggo, P. A., Jackson, S. P., and Doherty, A. J. (2002) *Science 297*, 1686−1689.
20. Petit, M. A., and Ehrlich, S. D. (2000) *Nucleic Acids Res. 28*, 4642−4648.
21. Sriskanda, V., Schwer, B., Ho, C. K., and Shuman, S. (1999) *Nucleic Acids Res. 27*, 3953−3963.
22. Kodama, K., Barnes, D. E., and Lindahl, T. (1991) *Nucleic Acids Res. 19*, 6093−6099.
23. Sambrook, J., Fritsch, E. F., and Maniatis, T. (1989) *Molecular cloning: a laboratory manual*, 2nd ed., Cold Spring Harbor Laboratory, Cold Spring Harbor, NY.
24. Yang, J., Gunasekera, A., Lavoie, T. A., Jin, L., Lewis, D. E., and Carey, J. (1996) *J. Mol. Biol. 258*, 37−52.
25. Sriskanda, V., and Shuman, S. (2001) *Nucleic Acids Res. 29*, 4930−4934.
26. Ho, C. K., Van Etten, J. L., and Shuman, S. (1997) *J. Virol. 71*, 1931−1937.
27. Nakatani, M., Ezaki, S., Atomi, H., and Imanaka, T. (2002) *Eur. J. Biochem. 269*, 650−656.
28. Doherty, A. J., Jackson, S. P., and Weller, G. R. (2001) *FEBS Lett. 500*, 186−188.
29. Weller, G. R., and Doherty, A. J. (2001) *FEBS Lett. 505*, 340−342.
30. Lorenz, M. G., and Wackernagel, W. (1994) *Microbiol. Rev. 58*, 563−602.
31. Dubnau, D. (1999) *Annu. Rev. Microbiol. 53*, 217−244.

BI0355387